

Spring 2015

Gene Expression of Tissue-Engineered Distal Phalanx Models Utilizing Polymer Scaffolds with Hydroxyapatite and Beta-Tricalcium Phosphate

Kristrun H. Kristinsdottir
The University Of Akron, khk5@zips.uakron.edu

William J. Landis Ph.D.
The University Of Akron, wlandis@uakron.edu

Robin Jacquet M.S.
The University Of Akron, rmj@uakron.edu

Please take a moment to share how this work helps you [through this survey](#). Your feedback will be important as we plan further development of our repository.

Follow this and additional works at: http://ideaexchange.uakron.edu/honors_research_projects

 Part of the [Polymer Chemistry Commons](#)

Recommended Citation

Kristinsdottir, Kristrun H.; Landis, William J. Ph.D.; and Jacquet, Robin M.S., "Gene Expression of Tissue-Engineered Distal Phalanx Models Utilizing Polymer Scaffolds with Hydroxyapatite and Beta-Tricalcium Phosphate" (2015). *Honors Research Projects*. 74.

http://ideaexchange.uakron.edu/honors_research_projects/74

This Honors Research Project is brought to you for free and open access by The Dr. Gary B. and Pamela S. Williams Honors College at IdeaExchange@UAKron, the institutional repository of The University of Akron in Akron, Ohio, USA. It has been accepted for inclusion in Honors Research Projects by an authorized administrator of IdeaExchange@UAKron. For more information, please contact mjon@uakron.edu, uapress@uakron.edu.

Gene Expression of Tissue-Engineered Distal Phalanx Models Utilizing Polymer Scaffolds

with Hydroxyapatite and β -Tricalcium Phosphate

Kristrun Kristinsdottir

9871:497

Abstract:

Tissue engineering is a scientific methodology that provides the means for fabrication of vital tissues in a laboratory with the ultimate goal of translating the tissue to a patient in a clinic. It is a desirable technique in clinical medicine because it eliminates the need for patient tissue grafts and transplants, which have the potential for donor site morbidity and rejection. In tissue engineering, the scaffolding material, typically a polymer upon which tissue is grown, is important. The goal of this research is to investigate optimization of tissue-engineered polymer scaffold constructs for cell proliferation and gene expression. This work includes an analysis of scaffold type to determine the appropriate engineered materials for growing human periosteum. Many scaffolding materials have been investigated for tissue-engineering purposes; however, the present study will be examining novel scaffolds for growing periosteum, those scaffolds being composed of hydroxyapatite (HA) or beta-tricalcium phosphate (β-TCP) with polylactic acid/polycaprolonic acid [P(LA/CL)]. To conduct this analysis, histology of tissue-engineered constructs will be utilized to determine cell proliferation, and reverse transcription-quantitative polymerase chain reaction (RT-qPCR) will be applied to determine gene expression of construct cells. Results will be compared to determine differences in fold-change expression levels of several genes of interest that may be affected by the two different scaffolds. The initial findings of the study showed that there were few significant differences in gene expression between the scaffolds composed of HA or β-TCP.

Introduction:

Tissue engineering is an experimental technique used to augment, replace, and repair congenitally defective, damaged, or missing tissues. Initially proposed by Langer and Vacanti in 1993, tissue engineering has become widely implemented to regenerate a variety of tissues, including mineralized connective tissues such as cartilage and bone.¹ Before tissue engineering

was developed, the common method of replacing or repairing tissues involved prosthetics, transplanting foreign tissues, or grafting tissues from other parts of the body of the patient. While still practiced, prosthesis, transplantation, and grafting often lead to tissue rejection and inflammation as well as donor site morbidity. This study will be examining novel scaffolds as potential improvements for tissue engineering of bone and ultimately for advancing methods beyond transplantation and grafting.

The tissue engineering of constructs involves three principle aspects, a source of cells, an appropriate and biocompatible scaffold material, and possible application of cytokines and growth factors. The major cells and tissues involved in this study include bone, cartilage, and periosteum.

The human skeleton, which gives the body a rigid framework, is composed principally of bone. In addition to serving as an attachment point for soft tissues, the skeleton provides a means for locomotion, furnishes protection to otherwise vulnerable organs such as the brain and the lungs, and acts as a calcium reservoir, depositing or absorbing calcium as the body demands. Bone contains other ions, such as sodium and phosphorous, and can also accumulate or release these to maintain ionic homeostasis in the fluids of the body.²

The process of bone growth is referred to as ossification. There are two types of ossification: endochondral and intramembranous. They are distinct from each other, but bones formed by the two different processes exhibit the same histologic structures³ (to be explained later).

*Endochondral ossification*³ is the process by which most bones of the body develop. The endochondral course of growth involves the formation of a temporary hyaline cartilage model. This model precedes bone formation and allows bone to increase in size by interstitial and appositional means. The chondrocytes in hyaline cartilage divide, mature, and hypertrophy (swell), then begin to calcify. The calcified matrix serves as the structural framework for the

development of bone. Bone is generated as a result of the invasion of hypertrophic cartilage by vascularity, which brings in new cells that erode the chondrocytes and replace them with osteoblasts. As cartilage is replaced by bone material, a surrounding layer of connective tissue called periosteum is formed simultaneously at the bone surface. Periosteum contains the cells needed to grow bone, including osteoprogenitor cells of both chondrocytes and osteoblasts, again, at the bone surface. This process is called intramembranous, or appositional, ossification.

*Intramembranous ossification*³ occurs when bones grow not from a cartilage model, but from a precursor connective tissue called mesenchyme. Some mesenchyme cells, known as mesenchymal stem cells, differentiate into osteoblasts, which secrete extracellular matrix proteins that have the capacity to induce bone formation. Once surrounded by this matrix and upon its subsequent calcification, osteoblasts become enclosed or reside within small cavities termed lacunae. At this point osteoblast function is diminished, and operationally these cells are considered osteocytes. Osteocytes now begin to establish connections with neighboring osteocytes, osteoblasts, and osteoclasts (bone-resorbing cells) through multiple canaliculi, small canals that provide a means for cell-to-cell communication. This process of ossification forms the mandible, maxilla, clavicles, and flat bones of the skull.

Cartilage is a specialized type of connective tissue often associated with bone. The firm consistency of the extracellular matrix secreted by chondrocytes, or cartilage cells, gives this tissue the ability to bear mechanical stress without permanent distortion.³ This property of cartilage occurs because its matrix is rich in glycosaminoglycans and proteoglycans, which interact with collagen and elastic fibers to impart shock-absorbance. This tissue also provides a sliding area for joints and facilitates bone movement. There are three forms of cartilage, hyaline (the most common form), elastic, and fibrocartilage. Each type maintains certain individual properties, but all three share the fact that they are avascular and must be nourished by diffusion

of nutrients from surrounding capillaries. These capillaries are found in adjacent connective tissue, known as perichondrium. Chondrocytes play an essential role in the development of long bones. Every long bone contains a growth plate, which is responsible for interstitial bone growth. The growth plate is composed of four zones of cartilage. The zone of reserve cartilage is located closest to the joint, and is made up of resting chondrocytes. Immediately below the reserve cartilage is the zone of proliferating chondrocytes. This layer consists of cartilage cells in the process of dividing and forming cellular columns. The nuclei and cytoplasm of these chondrocytes increase in size and the cells swell, creating the zone of hypertrophy. The hypertrophied cells begin to break down and form thin plates of calcified cartilage as noted above. Below this calcifying layer, bony material is deposited on the calcified matrix, creating a zone of provisional ossification. This zone is ultimately responsible for the growth of the long bone, as it is the template or stratum where the new bone forms.³

Periosteum is a thin membrane, both fibrous and cellular, that covers the surfaces of all bones. The outer fibrous layer is composed in part of fibroblasts and collagen, the collagen extending through the periosteum and into the bone matrix. These Sharpey's fibers, as the collagen fibers are often called, provide the periosteal layer with a strong anchor and tight bond to the bone. The inner cambium layer of the periosteum is cellular, made up of fibroblast-like cells known as osteoprogenitor cells. These cells, as their name suggests, have the potential to divide and differentiate into osteoblasts, the bone-forming cells. The progenitor cells have the ability to respond to various chemical signals and can develop into chondrocytes if necessary. The periosteal layer is highly vascularized, and it is responsible for providing nourishment to the bone. The periosteum plays an important role in bone remodeling and is responsible for the appositional growth of bone as described above.⁹

The Landis Laboratory has previously investigated gene expression of human periosteum applied to certain polymer scaffolds for tissue engineering.^{1,4,5,6} This work involved use of human donor cadaveric tissue that was composed of periosteum (bone and cartilage cells as just detailed). The periosteum was wrapped about polymer scaffolds and incubated in athymic (nude) mice for times up to 60 weeks. The periosteum-scaffold constructs were retrieved after implantation and analyzed in part for their gene expression using the method of reverse transcription-quantitative polymerase chain reaction (RT-qPCR) analysis. Constructs are assemblies that consist of cells or tissues applied to a substrate or scaffold, commonly a polymer. These constructs are then used to augment, replace, and repair tissues, as discussed earlier. The purpose of the scaffolding for engineering the tissues is to guide cell attachment, migration, proliferation, differentiation, and tissue regeneration.

In the current research, a similar project will be undertaken; however, it will examine scaffolds that have not previously been studied. The purpose of investigating these scaffolds is to determine which mineral component increases gene expression of bone- and cartilage-specific genes. Periosteum will be wrapped about polymer scaffolds of 70% hydroxyapatite/30% polylactic acid/polycaprolinic acid (50/50) [HA70%P(LA/CL)] and 3% -tricalcium phosphate/97% polylactic acid/polycaprolinic acid (50/50) [TCP3%P(LA/CL)]. As stated, the purpose of the scaffolding is to guide cell and tissue growth. The scaffold material must be porous, to allow nutrients and metabolites to penetrate through it, and it may be conducive to vascularization of the tissue.²

Often, PLA and PCL are used as the basic polymers comprising tissue-engineering scaffolds. They are desirable because of their ability to degrade and resorb in the body, avoiding long-term complications or rejection since they are biocompatible.² These materials can be combined with other components, such as HA or -TCP minerals (in the case of the current research) to aid in

the engineering of new tissue and impart strength to the scaffolds. Combination with these minerals may have effects on the growth and gene expression of the tissue as two possible outcomes of interest in this study.

Work in other laboratories has been done examining HA as a component of tissue-engineering scaffolds. With HA being a major component of the inorganic portion of bone, HA-laden scaffolds can serve as a site for new bone deposition. As a synthetic polymer with HA begins to disappear on resorption, the mineral has the ability to contribute to and integrate into the newly forming bone.² In one study, a porous HA/PLLA scaffold and a pure PLLA scaffold were seeded with osteoblasts to determine differences in a number of cell parameters as a function of HA presence. Results ultimately favored the HA-containing scaffold: The researchers found that the HA scaffold led to a larger percentage of cell survival, more uniform osteoblast distribution with deep penetration into the scaffold, and higher expression levels of the bone-specific genes, bone sialoprotein (BSP) and osteocalcin (OC). These results indicate that HA as a component of a tissue-engineering scaffold imparts osteoconductivity,² meaning the mineral is able to help guide the regeneration and repair of the natural bone. HA is useful in tissue engineering because of its osteoconductive properties, but it may not be useful in other situations. For example, when used simply as a bone graft without any engineered tissue, HA is minimally absorbed by the body, and its presence blocks any formation of new bone and prevents bone remodeling. This result often leads to reduced stability at the site of the graft and permanent stress concentration in that area.⁸

- TCP is the other mineral component used to create the scaffolding in this research project. Little work has been done investigating the function of -TCP when seeded with cells or tissues, but studies have examined uses of this polymer simply as a bone grafting material. As a bone graft, -TCP holds an equivalent balance between scaffold absorption and bone formation. As a biodegradable ceramic material, it has the ability to supply both calcium and sulfate ions to the

body as well as provide a solid scaffold structure for bone regeneration. For these reasons, - TCP is useful as a bone graft, but in terms of tissue engineering, it lacks osteoconductivity and osteogenicity, which may hinder its application in the current study.⁸ Osteogenicity is a function of living bone cells in the scaffold to contribute to bone healing and remodeling.

The periosteum used in this research was obtained from the femur of a deceased 16-year old male. In addition to periosteum, chondrocytes were taken from the donor joint. Periosteum was dissected into small strips that were wrapped about either the HA- or -TCP-scaffolds, shaped as rectangular solids, approximately 1 X 0.5 X 0.5 cm. The construct to be fabricated in these studies is a model of a human distal phalanx. This model consists of a midshaft (HA- or -TCP-scaffolds wrapped with periosteum) and one cartilage endplate. The endplate in the model is constructed of chondrocytes seeded onto polyglycolic acid (PGA) sheets, approximately 1 X 1 X 0.2 cm. Periosteum-wrapped midshafts were prepared by placing the constructs in M199 culture medium at 37°C at 5% CO₂ for five days. To prepare chondrocyte-seeded PGA sheets, chondrocyte suspensions in Ham's F12 medium were seeded onto PGA sheets and incubated for four hours at 37°C and 5% CO₂ to allow cells to adhere to PGA. At this point, additional Ham's F12 medium was added, and samples were incubated for five days. After incubation, chondrocyte-seeded PGA sheets were sutured with 5.0 Vicryl thread to the ends of the periosteum-wrapped scaffolds. The complete model constructs were placed in Petri dishes and incubated in M199 culture medium at 37°C at 5% CO₂ for 24 hours. Following incubation, the constructs were implanted in nude mice and grown for periods of 5 and 20 weeks. Nude mice have no thymus and therefore a suppressed immune system. As a result, these animals can accept and grow tissues from other species since the mice have a compromised immune system. The animals may then serve as bioreactors to assist in understanding the development of the implanted human constructs used in this study. After the 5- and 20-week incubation periods, the

constructs were retrieved from the mice. They were ground to a powder in liquid nitrogen, and their RNA was isolated.

Remaining research will involve investigation of construct gene expression using RT-qPCR. Five genes will be of interest: BSP, type I collagen, type II collagen, OC, and osteonectin (ON). BSP is important to examine because it is a prominent component of mineralized tissues such as bone and calcifying cartilage. BSP is composed of 327 amino acids, with the mature protein weighing 33-34 kDa.¹⁴ The protein contains long stretches of glycine and glutamic acid residues, which are believed to play a role in the ability of BSP to serve as a nucleation site for HA.⁷ Another prominent gene expressed by cells of mineralizing tissues is type I collagen. The most abundant form of collagen in the body, type I collagen as a protein makes up the organic portion of bone, for example, and imparts tensile strength within this tissue. Type I collagen protein consists of three coiled subunits: two $\alpha 1$ chains and one $\alpha 2$ chain. Each chain is made of 1039 amino acids,¹⁷ and the three chains wind around one another to form a right-handed helix. Triple helices are the primary structural units of collagen fibers and occur because of the large number of glycine, proline, and hydroxyproline residues.¹⁰ In addition to type I collagen, the gene expression of type II collagen will be studied. Type II collagen protein, at 1487 amino acids long,¹⁵ is the principal component of hyaline cartilage, (articular, growth plate, nasoseptal, and costal cartilage), elastic cartilage (auricular), and fibrocartilage (joining tendon or ligament to bone). Articular cartilage covers bone surfaces at articulating joints, and the chondrocytes used in the current research were obtained from this type of joint. OC is another gene of interest. The counterpart of this gene is a noncollagenous protein found in most normally and abnormally mineralizing vertebrate tissues and often studied in tissue-engineered bone.² Numbering between 47 and 51 amino acids (depending on species), OC is a calcium-binding protein expressed abundantly in the organic matrix of bone.¹¹ Specifically, OC is expressed and secreted by

osteoblasts and chondrocytes and therefore can be used as a marker for bone and cartilage formation. Expression of the ON gene, which leads to production of its glycoprotein in bone that binds calcium with high affinity, will also be examined. ON is a 32 kDa bone-specific protein, coded for by 286 amino acids.^{12,13} It has a high affinity for calcium ions, HA, and type I collagen, which leads to the hypothesis that ON may play a role in regulating bone mineralization.¹³ However, some studies have shown that ON glycoprotein inhibits HA formation and growth.⁷

The expression of these genes of interest in the tissue-engineered constructs will be compared to determine which scaffold type yields an engineered tissue with higher levels of human bone and cartilage genes. The engineered tissue must be as similar as possible to the endogenous human tissue, so as to minimize the potential that the recipient may reject the new tissue.

In addition to analyzing the gene expression in the tissue-engineered constructs, their histology will be studied. Histology provides a means to examine the morphology of tissue specimens and can aid in determining the location and relative amounts of their various components.⁹ In medicine, histopathological examination can indicate a disease state or other abnormality if irregular cells or tissues are observed within a specimen. A multitude of different histological stains can be employed, and each can be used to elucidate a different type of cellular component. A drawback of using traditional histology to examine tissues is that typically tissues are chemically fixed, and the fixation process precludes investigations of dynamic events and metabolic functioning.

To prepare a tissue for histologic examination, the tissue must be properly fixed. Fixation is the preservation of structure and molecular composition of tissues. Ideally, tissues should be fixed as quickly as possible on retrieval from a sample. Fixation avoids tissue degradation that normally occurs by enzymatic or bacterial action at the point of tissue death. Various chemical fixatives are available for tissue preservation. Fixatives act by cross-linking proteins, thus

stabilizing the tissues.⁹ After fixation, the tissue must be embedded in a solid medium for sectioning. There are different ways to embed a sample depending on which type of microscopy is being used ultimately to examine the tissue. Paraffin wax is used to embed samples that will be examined with light microscopy, and plastic resin is used to embed those to be viewed by electron microscopy. Once the tissue is embedded, it may be sectioned. Paraffin sectioning involves cutting tissues into extremely thin (1-10 μm) slices with an instrument called a microtome. Sections are collected with forceps, floated on water, and transferred to glass slides.⁹

Another method available to prepare tissues is rapid freezing, in which they are fixed by being quickly frozen and subsequently sectioned with a cryostat. Rapid freezing is useful in studying sensitive enzymes, small molecules, lipids, or specimens that must be examined rapidly, such as tissues removed during surgery and in a non-chemically fixed state.⁹

Once transferred to glass slides, the tissue sections are stained. Various types of stains can be employed to provide information about different structures within the tissue.⁹ The stain used in the current experiments is toluidine blue (T-blue), a basic dye that has a high affinity for acidic cellular components and general cellular morphology. With T-blue staining, chondrocytes stain pink and periosteum stains blue for the studies here.

A model of bone growth and development is applicable to understanding tissue-engineered bone in this project. In Figure 1, the histological image illustrates how growth of a long bone occurs.³ As stated previously, long bone growth occurs through

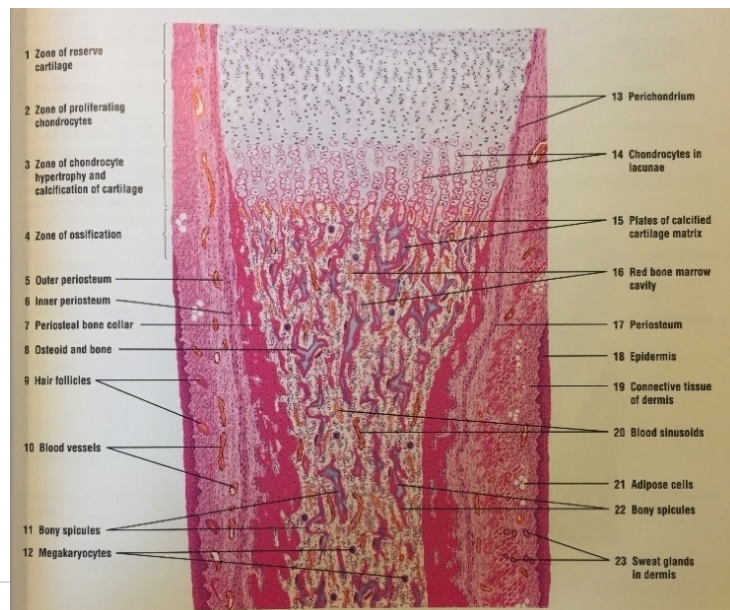


Figure 1. Taken from reference 2. A histologic image illustrating how long bone growth occurs. The various zones of growth and cell types are labeled.

endochondral ossification. Growth plates constitute the ends of long bones of the body and are responsible for longitudinal bone growth. For an explanation of the growth plate, see Page 5. Figure 1 shows the zone of reserve cartilage (1), the zone of proliferating chondrocytes (2), and the zone of chondrocyte hypertrophy and calcification (3). Ossification (4) occurs immediately below the zone of calcified cartilage, and bony material is deposited on the plates of calcified cartilage matrix. The diaphysis of the bone is covered by a periosteal layer (also previously explained) and is responsible for appositional growth of bone. Histological examination can help illustrate all these various bone and cartilage regions and provides a method for close investigation of tissue.³

As with all research, the current study does not come without experimental limitations. For example, in order to determine the efficacy and validity of this method, rigorous and repeated tests and trials must be completed successfully, and these can frequently pose complications. Since live cells taken directly from a patient are not readily accessible, the tissues to be used in this project must be obtained, with appropriate permissions, from donor cadavers. Even when harvested within 24 to 48 hours after donor death, cells are occasionally not viable because of natural degradative processes. Testing of harvested cells applied to scaffolds must be done carefully and involves demonstration that the constructs develop in the same way as their normal tissue counterparts. Validation of the developing construct is provided by examining it after implantation and retrieval from the nude mouse, and this examination can be accomplished using the techniques of histology and RT-qPCR (as will be done in the current study). Absolute certainty in the ability of the construct cells to express the desired genes must be obtained and proven repeatedly, and this requirement is another limitation in the tissue engineering methodology. Further, in a typical clinical application for tissue engineering, cells from a living patient are used, but harvesting those cells may cause morbidity at the site of collection, a

possibility that also may limit the experimental approach. Constructs must then be grown in the patient, a procedure that can cause risk of erosion or migration of the implant, in addition to exposure to possible infection. All these factors are yet more constraints to the tissue engineering technique.

Despite the limitations that exist, this project may offer significant clinical benefits to patients. If completed successfully with mice and moved to human trials in the future, the work here could help grow tissues that individuals have lost, such as severed fingertips, or have had injured or damaged. The tissue-engineering regime outlined in this study would not only regrow impaired, defective, or absent tissues, but also grow them accurately as compared to their endogenous human tissue counterparts. This approach ensures that the correct scaffold is used to support cells and genes of interest closest to those appearing in normal human bone.

Materials and Methods

All protocols were obtained from the Landis Laboratory and are summarized below.

RT-qPCR preparation: Freeze-grinding samples

To grind tissue samples, a freezer mill (Model 6870, Spex, Swedesboro, NJ) was filled with liquid nitrogen an hour before use to provide for sufficient cooling time for the instrument. Constructs were thawed on ice after removal from the -80°C freezer. Samples were removed individually from respective tubes using clean tweezers, rinsed in diethyl pyrocarbonate (DEPC) water to prevent RNase activity, and quickly submerged in liquid nitrogen. Constructs were placed into grinding tubes, each containing a cylindrical magnet, and tubes were sealed with a cap. Once the tubes containing samples were in the freezer mill, cycles were run as follows: 15-min pre-cool and three grind cycles of 2 min each. Upon completion of each cycle, tubes were removed from the instrument. Ground construct powder was emptied into pre-labeled 50-mL cylindrical tubes, containing 3 mL of TRI reagent (guanidinium thiocyanate-phenol-chloroform,

Molecular Research Center, Cincinnati, OH), maintained at 4°C on ice. Each tube was shaken and vortexed briefly to ensure mixing of construct powder with TRI reagent. Samples in tubes were then homogenized (See below) or refrozen at -80°C and stored.

Homogenization and phase separation

Homogenization and phase separation of the samples was performed on only four samples at a time. Ground and powdered samples stored in TRI reagent were removed from the -80°C freezer and were thawed on ice, vortexing intermittently. Tubes were placed into a refrigerated μ SpeedFuge tabletop centrifuge (Savant, Midland, MI) and spun at 2000 rpm and 4°C for 8 min. Supernatant was transferred into three 1.5-mL centrifuge tubes containing 1 mL each. Each 1.5-mL tube was vortexed and left at room temperature for 4 min. Tubes were supplemented with 100 μ L bromochloropropane (BCP, functioning as a phase-separation reagent) per 1 mL of TRI reagent. Tubes were vortexed for one minute. Samples were placed on ice for 15 min and then centrifuged at 13,000 g and 4°C for 30 min. During centrifugation, the mixture separated into a lower red-colored phase (protein), a white interphase (DNA), and an upper aqueous phase (RNA). The upper phase was pipetted and transferred to a fresh tube and supplemented with an equal portion of isopropanol, which in the current experiment was 750 μ L. Next, two μ L of glycogen were added to each tube to function as an inert carrier, free of any host genomic material. Samples were stored in a -80°C freezer.

RNA wash

Samples were washed to remove impurities possibly present in their RNA. Samples were removed from the -80°C freezer and spun at 13,000 g and 4°C for 30 minutes. Each tube was properly oriented in the centrifuge well, ensuring that the tab of the tube aligned with the back mark of the well. Following centrifugation, alcohol was carefully poured off the pellet, which

was concentrated at the bottom of the tube and whitish in color. In some cases the pellet did not remain at the bottom of the tube, and instead it was loose and tended to slide when alcohol was being removed. In these cases, alcohol was pipetted carefully and discarded. Next, 1000 μL of 70% EtOH/DEPC water (35 mL ethanol and 15 mL DEPC water, stored at -20°C) were added, and each tube was inverted several times to wash the pellets. Tubes were spun at 13,000 g and 4°C for 5 min. The wash was carefully removed from the pellet by pouring, if possible, and discarded. After this, 500 μL of 70% EtOH/DEPC were then added to the tubes, again inverting and washing the pellet. Tubes were spun at 13,000 g and 4°C for 5 min, and wash was poured off. Last traces of liquid were removed with a pipette and tubes were dried under a heat lamp for 5 min. Next, 350 μL of lysis buffer (EZNA Total RNA Kit I, Omega Bio-Tek, Norcross, GA) were added to each sample, followed by 350 μL of 70% EtOH/DEPC water at room temperature, which was pipetted repeatedly to ensure proper mixing. Each sample was then placed on a HiBind RNA spin column seated in a 2-mL collection tube and centrifuged in an Eppendorf 5424 Centrifuge at 10,000 g for 60 sec (Eppendorf, Hauppauge, NY). The flow-through (FT) was discarded and the collection tube was reused in the next step, where 250 μL of RNA Wash Buffer I were added to each sample by pipetting directly onto the column, still seated in a 2-mL collection tube. Again, tubes were centrifuged at 10,000 g for 60 sec and FT was discarded. At this step, a stock solution of DNase I was created using the following recipe: 294 μL EZNA DNase I digestion buffer (obtained from the kit) mixed with 6 μL of RNase-free DNase I (Omega, Norcross, GA). RNA columns were placed into new 2-mL collection tubes, and 75 μL of the DNase solution were pipetted onto the center of the column membranes. The columns were then incubated at room temperature for 15 min. Then, 500 μL of RNA Wash Buffer I were added, tubes sat at room temperature for 2 min, and were spun at 10,000 g for 60 sec. FT was

discarded and collection tubes were reused, then 500 μL of RNA Wash Buffer II were added, and tubes were spun at 10,000 g for 60 sec. Before using RNA Wash Buffer II, the solution was diluted with ethanol and brought to room temperature. FT was discarded and the wash was repeated. After the second wash with RNA Wash Buffer II, columns were spun with the empty collection tubes at 10,000 g for 2 min to dry. Columns were placed in clean 1.5-mL centrifuge tubes, properly labeled. Next, 40 μL of DEPC water were added directly to the center of column membranes. Columns sat for 1 min, and then they were spun at 10,000 g for 2 min. RNA was now in each centrifuge tube, as the DEPC water removed it from the column.

Quantitation of RNA

Once RNA had been isolated and purified, it was quantitated. Spectroscopic analysis was performed using an Eppendorf Biophotometer 6131 (Eppendorf, Hauppauge, NY). A clean cuvette was obtained and filled with 50 μL of 1X TE Buffer. The 1X TE buffer was made by mixing 10 mM Tris (brought to pH 8.0 with HCl) with 1 mM ethylenediaminetetraacetic acid (EDTA). The purpose of this buffer was to solubilize RNA (or DNA) while protecting it from degradation. TE buffer was stored at -20°C . The Biophotometer was set to analyze RNA. The instrument was blanked with the cuvette containing TE buffer. The cuvette was removed and 1 μL of sample was added. After wiping the sides of the tube with a KimWipe to eliminate the possibility of error because of an unclean cuvette, the cuvette was inserted into the holder, and the “sample” button was pressed. Spectroscopic analysis provided data indicating how pure samples were and how much RNA was present in each sample.

Reverse Transcription

Reverse transcription was begun by creating a buffer mix. The amount of buffer needed was dependent on the number of samples being reverse-transcribed. A volume of 8.5 μL of buffer

was required for each tube. The number of tubes needed was calculated by adding together the number of samples, a negative control for each sample (no reverse transcriptase), and a buffer blank (no RNA). The buffer recipe was as follows (Life Technologies, Grand Island, NY): (per tube) 2 μL of 10X buffer, 4 μL dNTPs (dinucleotide triphosphates), 1 μL oligo dT, 1 μL random hexamers, 0.5 μL RNase inhibitor (RI). Reaction components were added in the order listed. After addition of all ingredients, tubes were gently vortexed and centrifuged to concentrate buffer mix. The amount of RNA and DEPC water added to each tube was equal to 10.5 μL , and one μg of RNA was needed for each reaction. Using concentration obtained from the spectrophotometry data, μL of RNA were calculated. DEPC water was added to 10.5 μL to account for total volume. With no more than six tubes at a time, tubes were labeled with sample number, experiment number, species, date, and cDNA. To clean tubes, DEPC water was added first, according to calculations detailed above. Second, 8.5 μL of buffer mix were added to each tube. RNA was added last to each tube. Tubes were vortexed and spun, then gently set into a 65°C heater for 5 min. Next, tubes were placed in a clean RNase-free rack at room temperature for 10 min. After allowing the tubes to sit at room temperature, 1 μL of reverse transcriptase was added to each tube (except for the negative controls) and mixed with the pipette tip. The tubes were allowed to sit at room temperature for an additional 10 min. Next, they were moved to the 37°C heater block for one hr. To destroy any RNA that may not have been reverse-transcribed, samples were placed at 95°C for 5 min, then cooled on ice. At this point, the tubes contained cDNA, and they were stored separately from RNA tubes at -80°C. In addition to reverse-transcribing samples, standard concentrations of control tissues were also reverse-transcribed. These were used to generate standard curves. 20 μL each of human tendon, meniscus, chondrocyte, and periosteum cDNA samples were mixed together, creating a stock

solution at 40 ng/μL. Because of the fact that the reverse transcriptase enzyme is only 80% efficient, 1 μg of RNA gave cDNA at a concentration of 40 ng/μL. From the stock solution, 60 μL of each standard concentration needed (20 ng/μL, 10 ng/μL, 5 ng/μL, 1 ng/μL, 0.5 ng/μL, 0.1 ng/μL, and 0.01 ng/μL) were created.

Quantitative Polymerase Chain Reaction

Following synthesis of cDNA from RNA samples, a quantitative polymerase chain reaction (qPCR) analysis was run to determine gene expression in the sample tissues. Before starting the qPCR, centrifuges to be used were pre-cooled to 4°C. cDNA samples were removed from the -80°C freezer, and primers were removed from a -20°C freezer. Following sample removal, they were maintained in a grid-like pattern on the ice while thawing, as it aided in organizing the pipetting of a plate. While samples and primers were thawing (around 30 min), the PCR instrument was turned. The program was set up by opening the 7500 software application, and creating and naming a new experiment. Under **Experiment Properties**, “7500 (96 wells),” “Quantitation—Relative Standard Curve,” “TaqMan Reagents,” and “Standard (2 hr to complete a run)” were selected. Under **Plate Setup**, the *Define Targets and Samples* tab was entered. Under *Define Targets*, the target primer for the gene to be run was added. For example, if running 18S rRNA, the target selected was *18S rRNA (Taq), FAM, NFQ-MGB*. Under *Define Samples*, both “Buffer Blank” and “Minus RT” were added, and all other samples, as well as positive controls, were input manually. If 18S rRNA was being determined, standard concentrations of 0.01 ng/μL-5 ng/μL were used. For all other genes, 0.1 ng/μL-20 ng/μL were chosen. Under the *Assign Targets and Samples* tab, all the wells on the plate to be used were selected. The appropriate target was added to the entire plate, and positive controls (run in triplicate), negative controls and buffer blank (singlets), and samples (duplicates) were entered

into the correct wells. Under **Run Method**, the *Tabular View* tab was opened, and “Reaction Volume Per Well” was changed from 50 μ L to 20 μ L. For 18S rRNA, “Number of Cycles” was changed from 40 to 35. For any other gene analysis, the number of cycles was left at 40. The reaction stage was set as follows:

For 18S:

	Holding Stage	Holding Stage	Cycling Stage	
Ramp Rate (%)	100.0	100.0	100.0	100.0
Temperature ($^{\circ}$ C)	50.0	95.0	95.0	60.0
Time	2:00	10:00	00:05	00:30

For all other genes:

	Holding Stage	Holding Stage	Cycling Stage	
Ramp Rate (%)	100.0	100.0	100.0	100.0
Temperature ($^{\circ}$ C)	50.0	95.0	95.0	60.0
Time	2:00	10:00	00:15	01:00

At this point, the computer software was ready to run once the reaction plate had been inserted.

Next, the master mix was created. The number of wells needed for the amplification reaction was calculated, and an additional 10% of the volume was supplemented to account for pipette carry-over. The number of wells needed on the plate included positive controls, negative controls, buffer blank, and samples. The master mix was created using the following recipe: (per well; a total amount was obtained by multiplying by the number of wells) 10 μ L TaqMan 2X (Life Technologies, Grand Island, NY), 1 μ L primer set, 8 μ L sterile H₂O, 1 μ L cDNA. Master mix was created in a 1.5-mL centrifuge tube, and tubes were stored at -80 $^{\circ}$ C until needed.

After the cDNA was thawed, it was centrifuged at 1,000 g for 1 min at 4 $^{\circ}$ C. An *Optical 96-Well Reaction Plate* (Life Technologies, Grand Island, NY) was placed in the holder, ensuring that nothing came in contact with the bottom of the plate. The holder in the rack was placed on

the mixer, and 19 μ L of master mix was added to the bottom of each well. After the master mix had been added, one μ L of cDNA was added to the side wall of each well, bringing the total volume per well to 20 μ L. The plate was sealed thoroughly with an optical adhesive film and squeegeed.

After the plate had been pipetted, it was processed. The plate was centrifuged in an Eppendorf 5810R centrifuge at 1200 rpm for 4 min at 4°C to pull cDNA into the master mix (Eppendorf, Hauppauge, NY). The plate was placed on a closed Eppendorf ThermoMixer (Eppendorf, Hauppauge, NY) at 1000 rpm for 5 min at 22°C to ensure thorough mixing of cDNA and master mix. The plate was centrifuged again at 1200 rpm for 4 min at 4°. The plate was placed into the instrument and *Start Run* was selected. Once the run was complete, the data could be analyzed.

Results

Quantitative Polymerase Chain Reaction Analysis

The current study examined expression levels of five different genes for the purpose of assessing whether they are affected by scaffolds containing either HA or -TCP. The genes of interest are type I collagen, type II collagen, BSP, OC, and ON. 18S rRNA, -actin, and P0 are used as reference controls since they are common housekeeping genes. Results were obtained by analyzing RT-qPCR data. The 18S rRNA gene is examined because it serves as an indicator of sample degradation, and the reliability of RT-qPCR data. -actin is used as a normalizing gene because it is assumed to be constantly expressed across a wide range of cell types. For this reason, all other genes are normalized to -actin during qPCR data analysis. Figures 2A-F show plots of the expression of each gene of interest after normalization with -actin. Figures 3A-B (5 and 20-week) present fold-change differences in the expression levels of these genes as a

function of scaffold type. For reference purposes to identify the tissues from which gene expression data were obtained, histological images are included as Figures 4-7.

Normalized Type I Collagen Expression

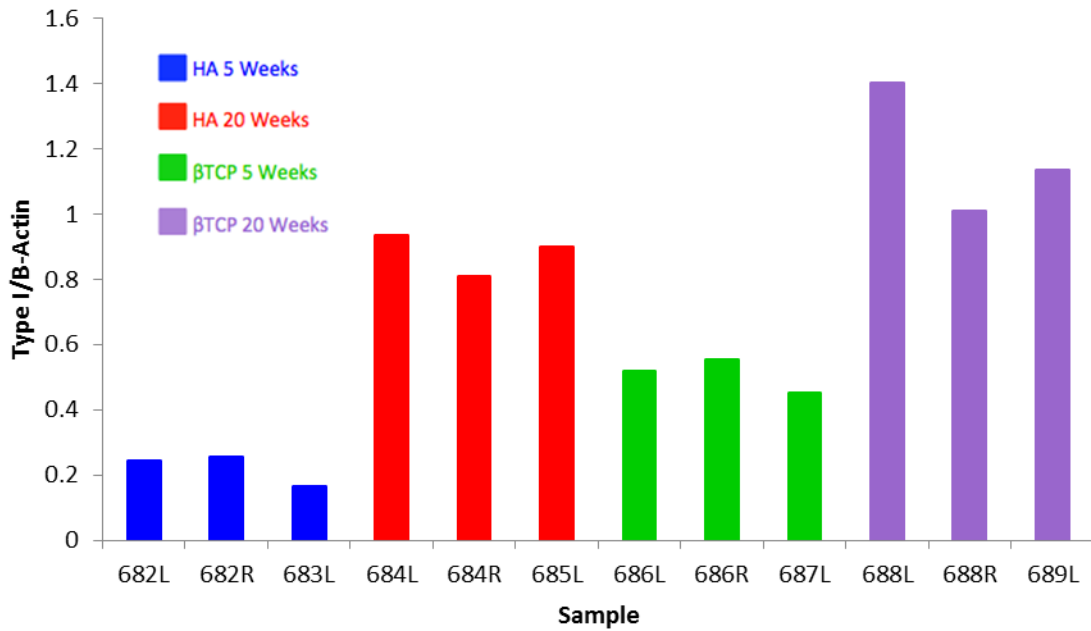


Figure 2A. Gene expression ratio of type I collagen normalized to β -actin. The colors represent the two different scaffold types used as well as the two different time points.

Normalized Type II Collagen Expression

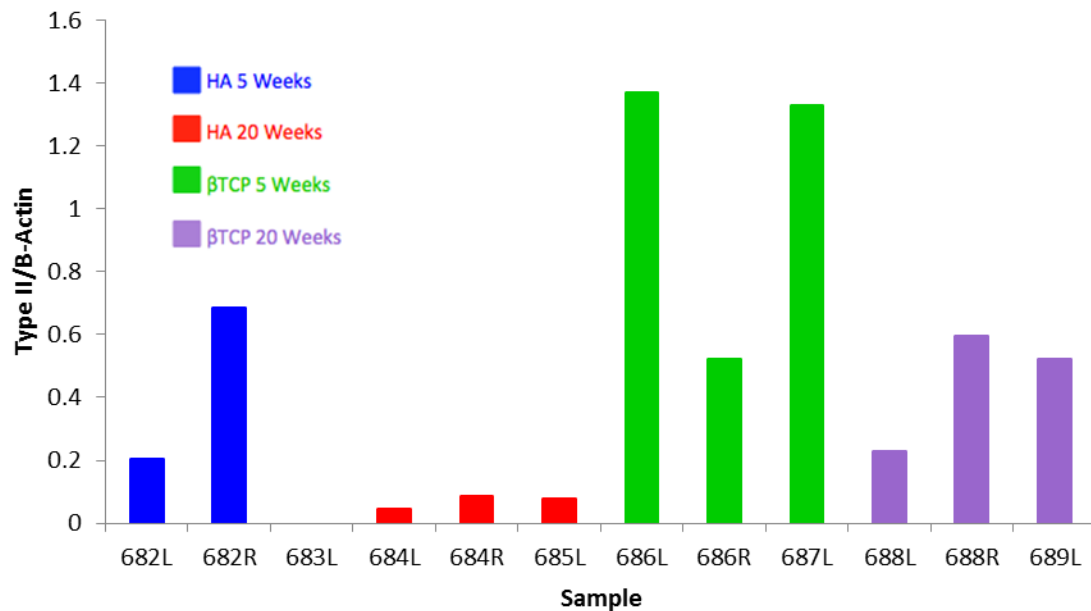


Figure 2B. Gene expression ratio of type II collagen normalized to β -actin. The colors represent the two different scaffold types used as well as the two different time points.

Normalized Bone Sialoprotein Expression

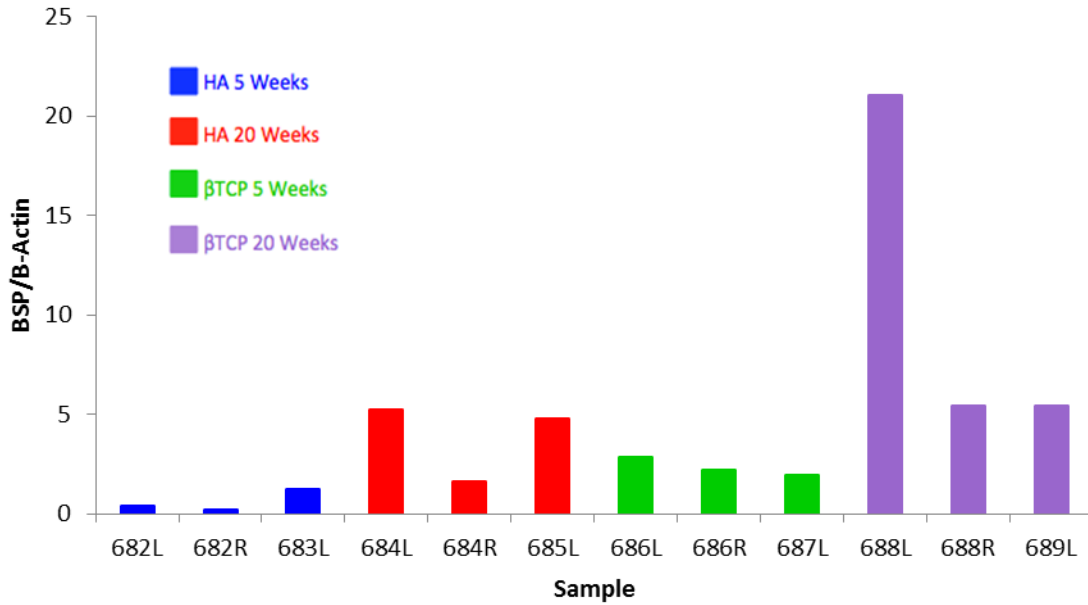


Figure 2C. Gene expression ratio of BSP normalized to β -actin. The colors represent the two different scaffold types used as well as the two different time points.

Normalized Osteocalcin Expression

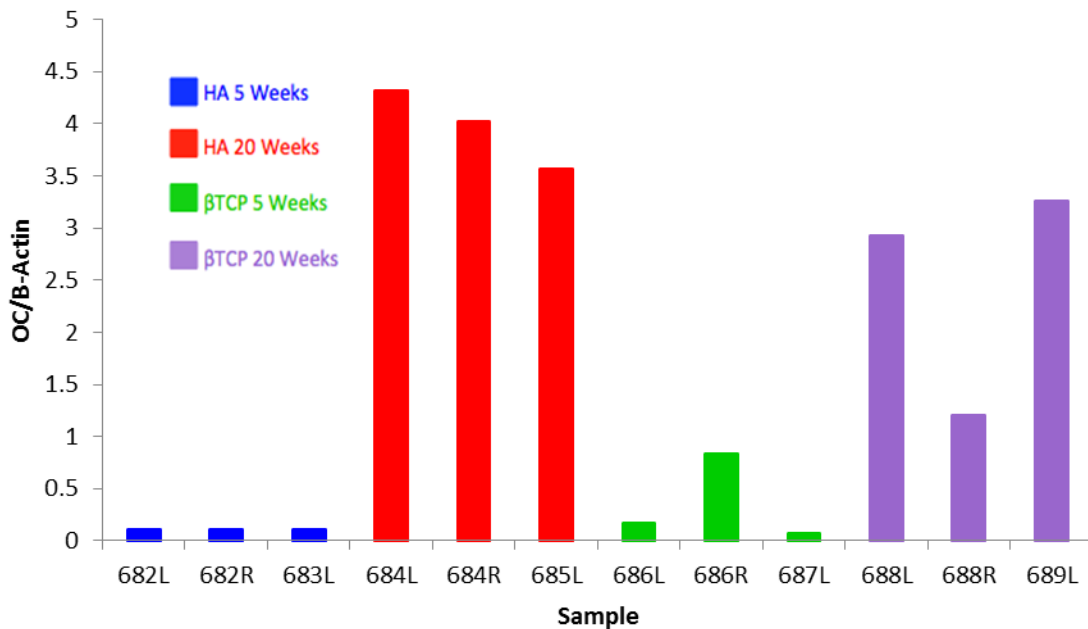


Figure 2D. Gene expression ratio of OC normalized to β -actin. The colors represent the two different scaffold types used as well as the two different time points.

Normalized Osteonectin Expression

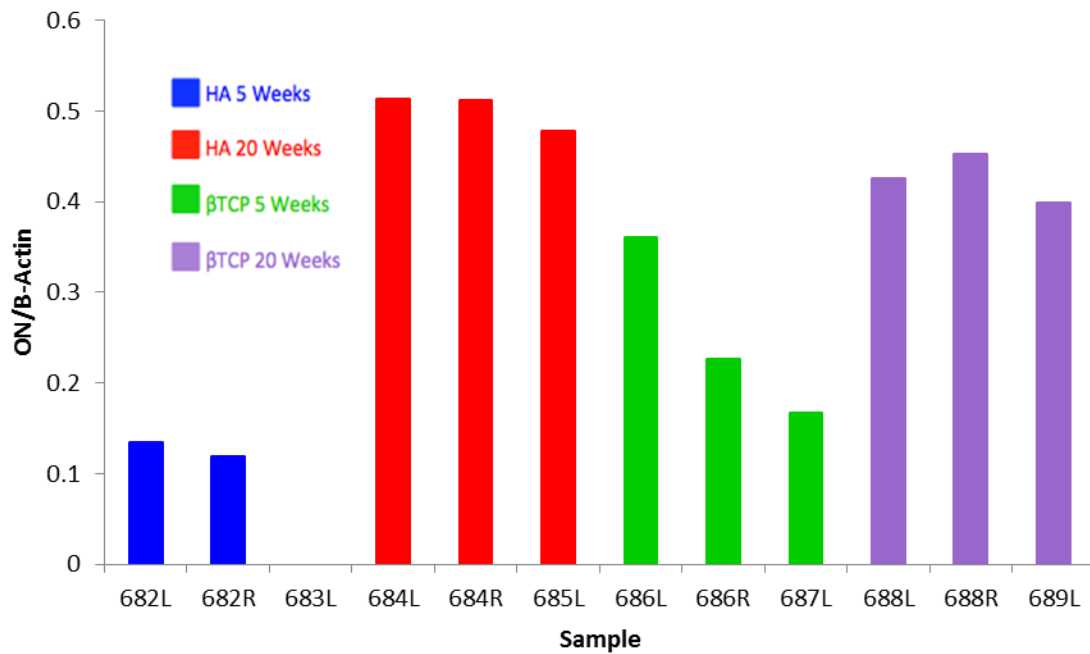


Figure 2E. Gene expression ratio of ON normalized to β -actin. The colors represent the two different scaffold types used as well as the two different time points.

Normalized PO Expression

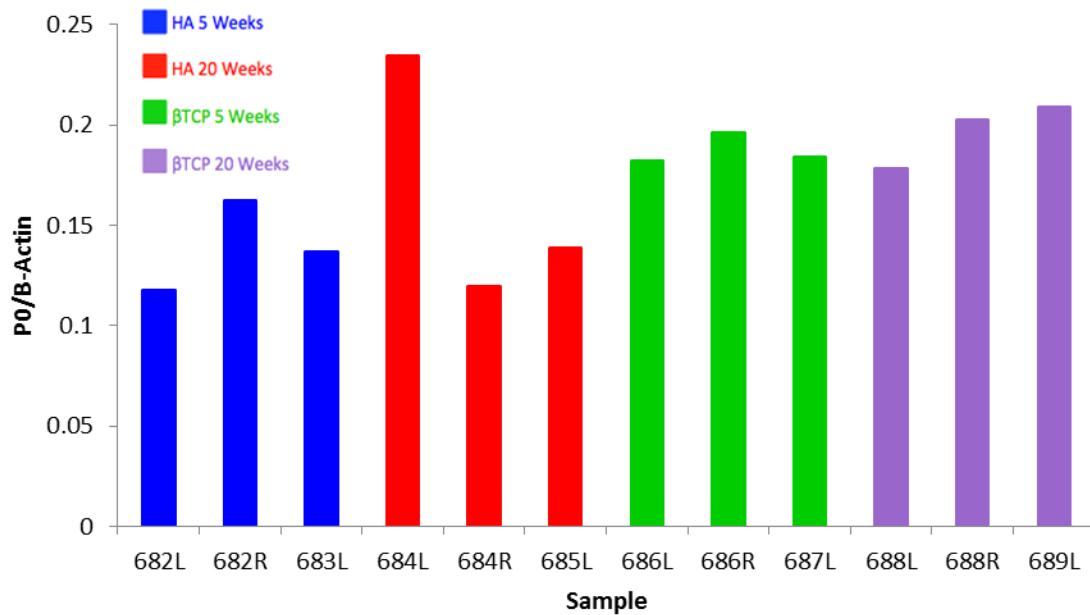


Figure 2F. Gene expression ratio of PO normalized to β -actin. The colors represent the two different scaffold types used as well as the two different time points.

Gene Expression Fold-Change in Tissue-Engineered Distal Phalanges after 5 Weeks of Implantation

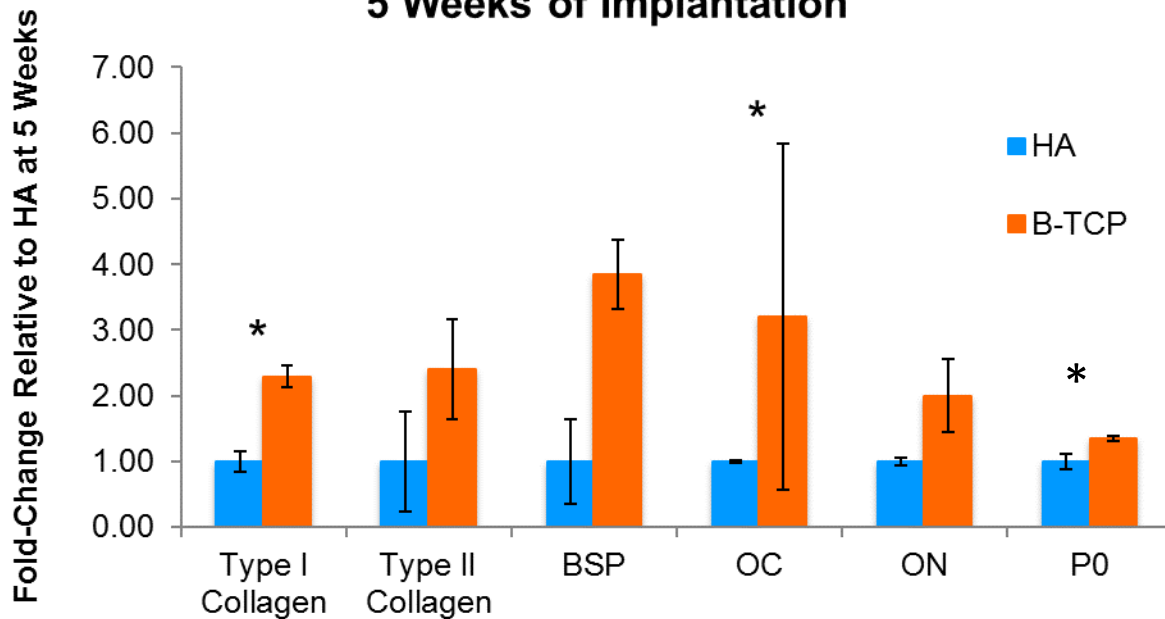


Figure 3A. Comparison by fold-change in distal phalanges developed on either HA or β -TCP scaffolds after 5 weeks of implantation in athymic mice. Statistically significant ($p < 0.05$) differences between HA and B-TCP specimens for a specific gene are shown by *. Data represent the mean value of three independent measurements and error bars represent standard error of mean values.

Figure 2A illustrates gene expression of type I collagen after being normalized to β -actin. Each bar represents a single normalized measurement taken for a given scaffold. From this plot, it may be observed that in general type I collagen expression increased with both scaffold types from 5 to 20 weeks of implantation and that expression with β -TCP scaffolds appeared to be consistently higher than that with HA scaffolds. The same conclusion can be drawn from Figure 2C, which shows BSP expression levels. Figure 2B presents type II collagen expression, which decreased with both scaffold types from 5 to 20 weeks of implantation, yet was higher at both time points with β -TCP scaffolding than with HA scaffolding. Figure 2D illustrates expression levels of OC and shows that expression increased with both scaffold types from 5 to 20 weeks of implantation. The same conclusion can be drawn from Figure 2E, which depicts expression

levels of ON. In both of these plots, it is observed that expression was consistently higher with the HA scaffolds than with β -TCP scaffolds.

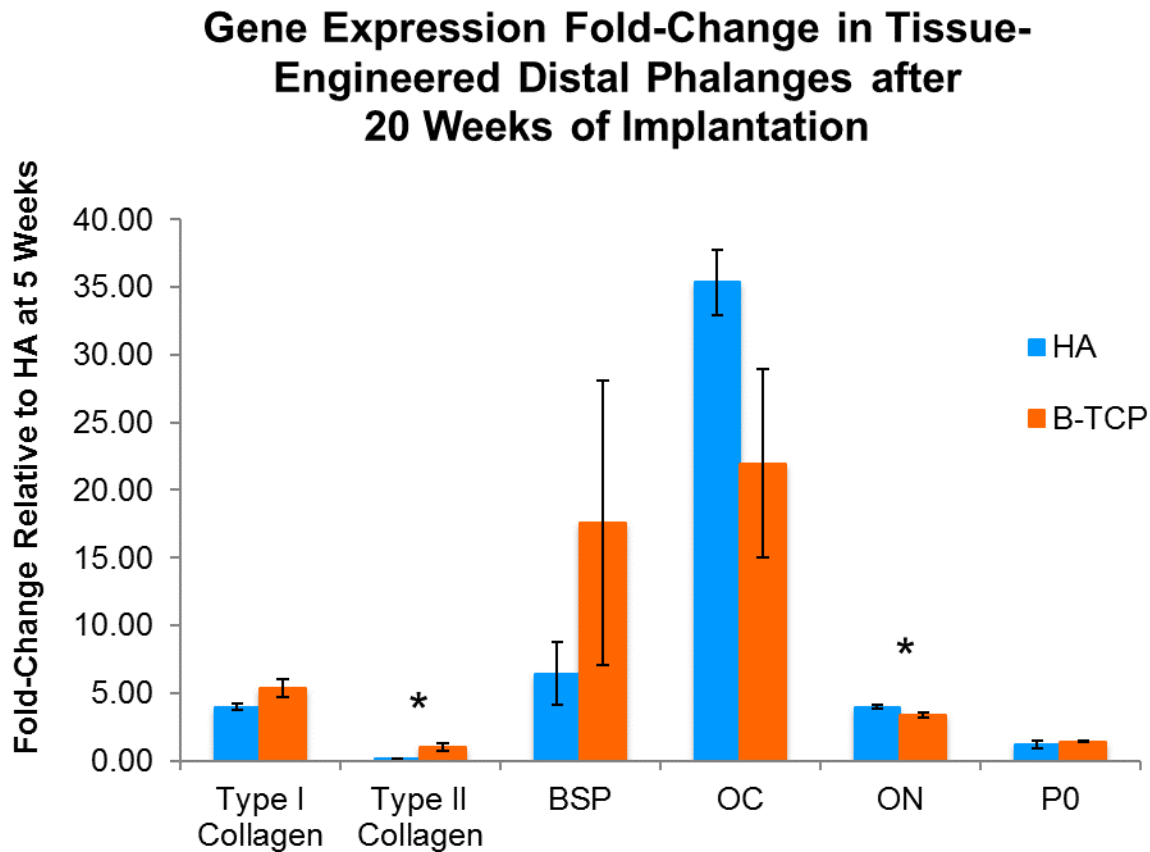


Figure 3B. Comparison by fold-change in distal phalanges developed on either HA or β -TCP scaffolds after 20 weeks of implantation in athymic mice. Statistically significant ($p < 0.05$) differences between specimens are shown by *. Data represent the mean value of three independent measurements and error bars represent standard error of mean values.

Statistical t-tests performed for $p < 0.05$ indicated that there were statistically significant gene expression differences for tissue grown on β -TCP compared to HA scaffolds after 5 weeks of implantation. The genes that were significantly different are shown in Figure 3A and included type I collagen and BSP. After 20 weeks of implantation (Figure 3B), a statistically significant difference was found for type II collagen, in which its expression on β -TCP scaffolds exceeded that on HA. In addition after 20 weeks of implantation, ON gene expression was statistically

significantly different (greater) when tissues were grown on HA scaffolds compared to -TCP scaffolds. Figures 3A-B suggest a trend in the expression of the genes of interest such that -TCP scaffolds induce greater expression than that of HA scaffolds. However, this conclusion is not supported by statistically significant data against -actin.

Figure 3A includes the analysis of a potential housekeeping gene, P0. Data from 5-week implanted scaffolds indicated that this gene was statistically significantly different when tissues were grown on -TCP and HA. In this case, P0 could not be used as the normalizing gene in this study, and instead -actin was selected in its place.

Histological Analysis

In addition to qPCR, histological examination was correlated with RT-qPCR analysis. Samples had been previously fixed, sectioned, mounted on slides, and stained with T-blue by others in the laboratory. The slides were viewed under a light microscope, and new images were obtained for this study.

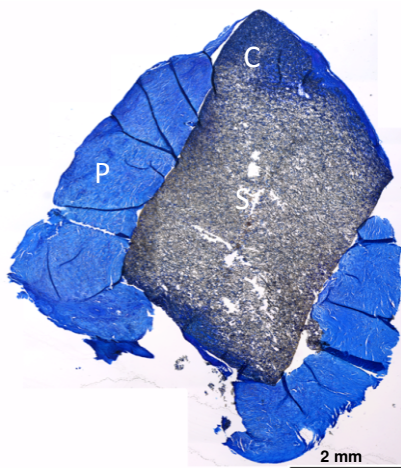
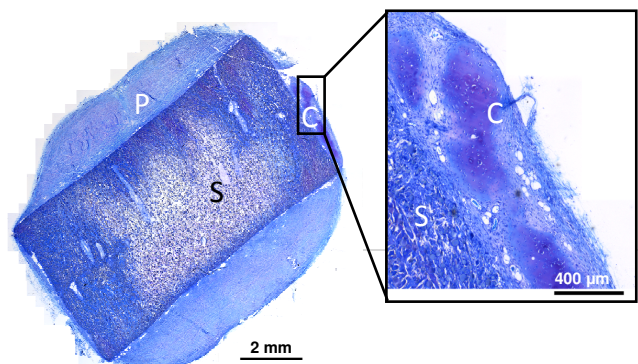


Figure 4 is an image taken of a 5-week implanted distal phalanx model developed on HA scaffolding. The scaffold (S) appears black and white, and the periosteum (P) wrapped around it is not stained blue. The top portion of the scaffold appears to contain chondrocytes (C) that likely migrated from the engineered PGA scaffold seeded with those cells. The overlying PGA scaffold has been lost or resorbed. Chondrocytes, however, from the PGA sheet appear to have migrated

somewhat into the HA scaffold.

Figure 5. A histological image showing a distal phalanx developed on an HA scaffold (S) and harvested after 20 weeks of implantation in an athymic mouse. The image (left) depicts the entire construct section, while the enlarged image (right) highlights a region of the construct PGA sheet seeded with chondrocytes (C). The periosteum (P) wrapped about the scaffold appears to have remained intact.



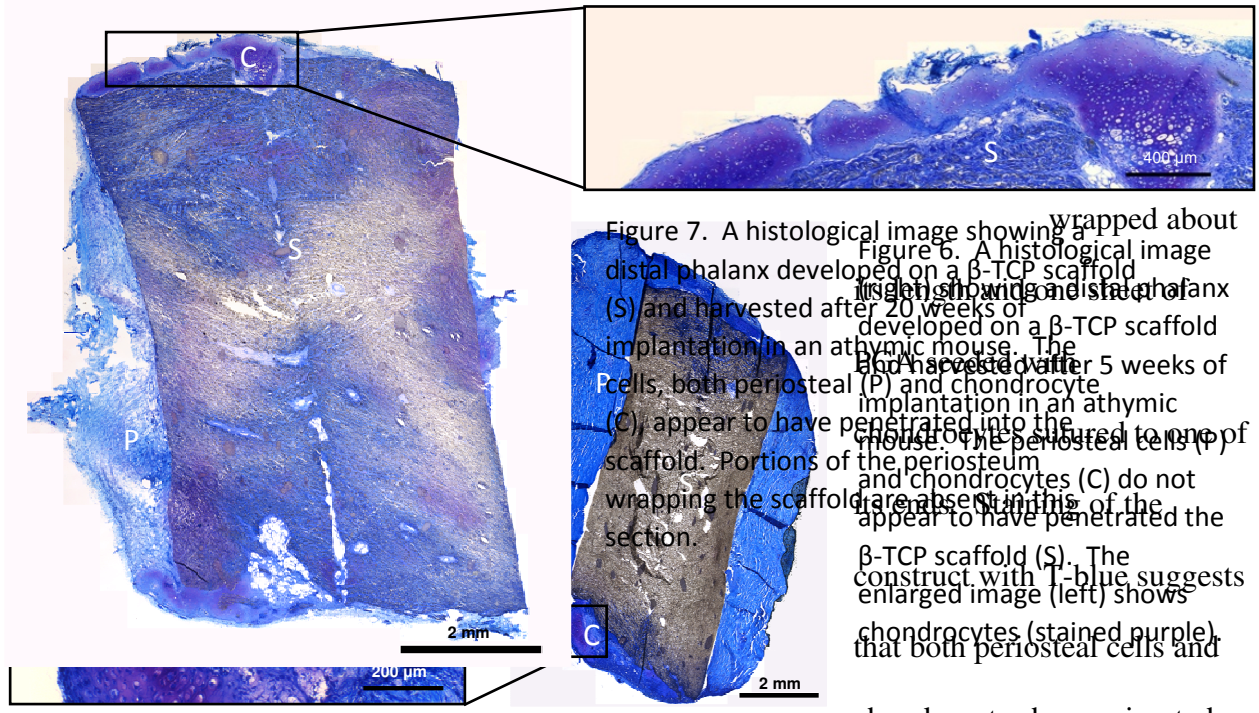


Figure 7. A histological image showing a distal phalanx developed on a β -TCP scaffold (S) and harvested after 20 weeks of implantation in an athymic mouse. The cells, both periosteal (P) and chondrocyte (C), appear to have penetrated into the scaffold. Portions of the periosteum wrapping the scaffold are absent in this section. Figure 6. A histological image showing a distal phalanx developed on a β -TCP scaffold harvested after 5 weeks of implantation in an athymic mouse. The periosteal cells (P) and chondrocytes (C) do not appear to have penetrated the β -TCP scaffold (S). The construct with T-blue suggests enlarged image (left) shows chondrocytes (stained purple), that both periosteal cells and

chondrocytes have migrated

into the HA scaffold (compare Figure 4 with its black HA scaffold).

Figure 6 shows a histologic image taken of a β -TCP sample at 5 weeks. As with the 5-week HA sample, the periosteal cells do not appear to have penetrated the scaffold. The chondrocytes, however, appear to have begun migrating into the scaffold by 5 weeks as they do in the 5-week HA sample (Figure 4).

Figure 7 is a histological image showing a β -TCP sample at 20 weeks. Much like the HA sample at 20 weeks shown in Figure 5, both periosteal cells and chondrocytes appear to have penetrated into the scaffold. The enlarged image shows a portion of the section where chondrocytes are concentrated, as evidenced by their purple staining.

Discussion and Conclusions

The goal of the current study was to examine a tissue-engineered distal phalanx model, composed in part by one of two different scaffold types, seeded with either an HA or β -TCP mineral component, and to observe possible changes in development and expression of certain genes as a function of the scaffold mineral. Each scaffold was wrapped about its length with a layer of human cadaveric periosteum. One scaffold end was sutured with a chondrocyte-seeded PGA sheet. The construct in this manner mimicked the morphology of a human distal phalanx.

The phalanx model specimens were previously designed and developed over 20 weeks of implantation in nude mice, and they were examined by histological means in other work. This report re-examined some of the same specimens by histology and then investigated possible changes in the expression of several genes as a function of scaffold type (either HA or β -TCP). The present study of such genes from tissue-engineered phalanx models supported by either HA or β -TCP scaffolds is novel. Little is known about any effects of a scaffold mineral on gene expression in bone- and cartilage-engineered constructs. The data obtained suggest that β -TCP scaffolds support increased gene expression of type I collagen, type II collagen, BSP, OC, and ON following 5 weeks of construct implantation in athymic mice. After 20 weeks of implantation in other athymic mice, the expression of type I collagen, type II collagen, and BSP appears to be enhanced by β -TCP scaffolding, while ON and OC are increased by HA scaffolding. Statistically significant changes in expression of only certain of these genes were

observed at either 5 or 20 weeks of implantation. The basis for these observed changes in gene expression are unclear with respect to the scaffold mineral component, but possibly the expression differences could be attributable to differences in mineral particle sizes. In this study, scaffolds of HA contained particles in the micron range, while scaffolds of β -TCP were in the sub-micron range. It could be possible that the smaller sized β -TCP particles, compared to HA, provide easier attachment, migration/penetration, and proliferation/differentiation for osteoblasts and chondrocytes in these constructs. In this regard, it is well documented that cells are responsive in gene expression and protein synthesis to the nature of the surfaces on which they reside. The surface characteristics including surface particle size, density, roughness, hydrophobicity, hydrophilicity, and other features affect cells substantially and up- and down-regulation of genes and proteins may normally result.¹⁹ In response to surface structure, different genes may be regulated in different ways, that is, some may be up-regulated while others may be down-regulated. This study demonstrates such up- and down-regulation in genes from the same construct, but again the fundamental basis for these observations is unclear.

The number of constructs examined in this work is relatively small and it is likely that more conclusive data could be obtained from an extension of this study with larger sample numbers. In addition, it is also likely that improved data could be generated with constructs implanted for periods greater than 20 weeks. Distal phalanx models without a mineral component have been implanted for up to 60 weeks in athymic mice in previous investigations.¹⁸ In these ways, the results presented here, showing changes in certain genes of distal phalanx models, may be supplemented and the interesting conclusion may be confirmed that a scaffold containing a mineral component can significantly influence gene expression and downstream protein synthesis and secretion.

Acknowledgments

I would like to thank Dr. William Landis for his support as my faculty mentor, Ms. Robin Jacquet for her endless knowledge and valuable help, Mr. Josh Bundy for assisting me with all steps of the project and providing the protocols for me, and Mr. Chris Burton for teaching me how to take histology images and stitch them together.

References

1. Wada, Y., Enjo, M., Isogai, N., Jacquet, R., Lowder, E., Landis, W. Development of bone and cartilage in tissue-engineered human middle phalanx models. *Tissue Engineering*, **2009**, *15*, 3765-3778.
2. Ma, P.X., Zhang, R., Xiao, G., Franceschi, R. Engineering new bone tissue *in vitro* on highly porous poly(-hydroxyl acids)/hydroxyapatite composite scaffolds. *The Journal of Biomedical Materials Research*, **2000**, *54*, 284-293.
3. Eroschenko, V.P. *diFiore's Atlas of Histology, with Functional Correlations*, 10th ed.; Lippincott, Williams, and Wilkins: Baltimore, 2005; pp. 65-89.
4. Matsushima, S., Isogai, N., Jacquet, R., Lowder, E., Tokui, T., Landis, W. The nature and role of periosteum in bone and cartilage regeneration. *Cells Tissues Organs*, **2011**, *194*, 320-325.
5. Shasti, M., Jacquet, R., McClellan, P., Yang, J., Matsushima, S., Isogai, N., Murthy, A., Landis, W. Effects of FGF-2 and OP-1 *in vitro* on donor source cartilage for auricular reconstruction tissue engineering. *International Journal of Pediatric Otorhinolaryngology*, **2013**, *78*, 416-422.
6. Landis, W., Jacquet, R., Lowder, E., Enjo, M., Wada, Y., Isogai, N. Tissue engineering models of human digits: Effect of periosteum on growth plate cartilage development. *Cells Tissues Organs*, **2009**, *189*, 241-244.

7. Hunter, G.K., Goldberg, H.A. Modulation of crystal formation by bone phosphoproteins: Role of glutamic acid-rich sequences in the nucleation of hydroxyapatite by bone sialoprotein. *Biochemical Journal*, **1994**, 302, 175-179.
8. Liu, B., Lun, D.X. Current application of beta-tricalcium phosphate composites in orthopaedics. *Orthopaedic Surgery*, **2012**, 4, 139-144.
9. Junqueira, L.C., Carneiro, J. *Basic Histology: Text & Atlas*, 10th ed.; McGraw-Hill Companies: New York, 2003; pp. 1-12, 135-159.
10. Lodish, H., Berk, A., Zipursky, S.L., et al. *Molecular Cell Biology*. 4th edition. New York: W. H. Freeman; 2000. Section 22.3, Collagen: The Fibrous Proteins of the Matrix.
11. Hauschka, P.V., Frenkel, J., DeMuth, R., Gundberg, C.M. Presence of osteocalcin and related higher molecular weight 4-carboxyglutamic acid-containing proteins in developing bone. *The Journal of Biological Chemistry*, **1981**, 258, 176-180.
12. Termine, J.D., Kleinman, H.K., Whitson, S.W., Conn, K.M., McGarvey, M.L., Martin, G.R. Osteonectin, a bone-specific protein linking mineral to collagen. *Cell*, **1981**, 26, 99-105.
13. Villarreal, X.C., Mann, K.G., Long, G.L. Structure of human osteonectin based upon analysis of cDNA and genomic sequences. *Biochemistry*, **1989**, 28, 6483-6491.
14. Ganss, B., Kim, R.H., Sodek, J. Bone sialoprotein. *Critical Reviews in Oral Biology and Medicine*, **1999**, 10, 79-98.
15. The UniProt Consortium. UniProt: A hub for protein information – CO2A1 Human. *Nucleic Acid Research*, **2015**, 43.
16. Murai, M., Sato, S., Fukase, Y., Yamada, Y., Komiyama, K., Ito, K. Effects of different sizes of β -tricalcium phosphate particles on bone augmentation within a titanium cap in rabbit calvarium. *Dental Materials Journal*, **2006**, 25, 87-96.

17. Landis, W.J., Silver, F.H. The structure and function of normally mineralizing avian tendons. *Comparative Biochemistry and Physiology Part A*, **2002**, *133*, 1135-1157.
18. Landis, W.J., Jacquet, R., Hillyer, J., Lowder, E., Yanke, A., Siperko, L., Asamura, S., Kusuhara, H., Enjo, M., Chubinskaya, S., Potter, K., Isogai, N. Design and assessment of a tissue-engineered model of human phalanges and a small joint. *Orthodontics and Craniofacial Research*, **2005**, *8*, 302-312.
19. Stevens, M.M., George, J.H. Exploring and engineering the cell surface interface. *Science*, **2005**, *18*, 1135-1138.

Appendix 1

Safety Considerations

Any scientific endeavor requires careful consideration to the issues of safety. It is critical to be familiar with the proper methods by which to handle and use chemicals and laboratory instruments.

When using the freezer mill to grind tissue samples, liquid nitrogen is utilized. Insulated gloves must be worn to protect skin from exposure to this compound.

This research makes use of human cadaveric tissue samples. It is imperative that gloves be worn at all times to avoid contact with the tissue and reduce exposure to possible human diseases from said tissue. In addition, the use of laboratory gloves ensures that samples themselves do not become contaminated. RT-qPCR is a very sensitive technique and will amplify any and all DNA present within a sample. Therefore, precautions such as wearing gloves (as stated above), using RNase Away® (Life Technologies, Grand Island, NY), and avoiding accidental contact such as breathing and sneezing on samples, will all help decrease the risk of sample contamination.

Caution must be taken during RNA isolation, reverse transcription, and qPCR, as the compounds used to perform the procedures are carcinogenic. Again, gloves must be worn when handling such chemicals, and any contact with the skin, mouth, or eyes should be avoided.